

# MD-Simulation of Molten LiCl; Self-Exchange Velocities of Li-Isotopes near Cl<sup>-</sup>-Ions

Isao Okada

Department of Electronic Chemistry, Tokyo Institute of Technology, Yokohama, Japan

Z. Naturforsch. **39a**, 880–887 (1984); received June 22, 1984

The experimental findings by Klemm et al. that in molten LiCl the isotope effect on the lithium mobilities increases with temperature and that the isotope effect between the two isotopically pure melts, i.e. <sup>6</sup>LiCl and <sup>7</sup>LiCl is greater than that in natural LiCl are reflected by the self-exchange velocities of the Li-isotopes near the Cl<sup>-</sup>-ions obtained by MD.

## I. Introduction

The isotope effect on the mobility of lithium in molten LiCl has intensively been studied by Klemm et al. [1–4]. One of the interesting features of their findings is that the isotope effect between pure <sup>6</sup>LiCl and <sup>7</sup>LiCl is greater than that in natural LiCl (<sup>6</sup>Li : <sup>7</sup>Li ≅ 7.42 : 92.58) and that both isotope effects increase with temperature.

In previous papers [5, 6] we have found that the mobilities of ionic melts are related to the separating motion of unlike ions which is obtainable from molecular dynamics simulations (MD). On the basis of this relation, phenomena such as the Chemla effect [5] and the maximum of electrical conductivity vs. temperature curves [6] can be interpreted.

The orthodox way of reproducing electrical mobilities is a method based on group velocity correlation functions suggested in such publications as [7–9]. However, this kind of method needs many MD time steps and is therefore very expensive for the moment. On the other hand, the method based on the separating motion of unlike ions does not necessitate so many time-steps. Thus, the purpose of the present study was to interpret the above mentioned experimental findings in terms of the separating motion of unlike ions as obtained by MD of molten LiCl.

## II. Simulation

The pair potentials of the Born-Mayer-Huggins type with the parameter values presented for LiCl

crystal by Tosi and Fumi [10] were used:

$$u_{ij}(r) = \frac{z_i z_j e^2}{4\pi \epsilon_0 r} + A_{ij} b \exp\left(\frac{\sigma_i^0 + \sigma_j^0 - r}{\varrho}\right) - \frac{c_{ij}}{r^6} - \frac{d_{ij}}{r^8}, \quad (1)$$

where  $z$  is the charge number,  $e$  the elementary charge,  $\epsilon_0$  the vacuum dielectric constant, and the parameter values  $A, b, \sigma, \varrho, c$  and  $d$  are those given in [10] (see, e.g. the table in [5]).

Although it has often been pointed out that the parameters given by Tosi and Fumi yield distances for the first peak positions of pair correlation functions of melts which are too short by 10–30 pm [11–13], these parameters were adopted here because they are known from many simulations to be good enough to reproduce various properties.

The side length,  $L$ , of the periodic cube was determined from the density:  $\varrho_d$  (g cm<sup>-3</sup>) = 1.8842 – 0.4328 × 10<sup>-3</sup> T (K) [14]. The number of ions in the cube was 216. The step time was 4 fs. Most of the MD runs were carried out with the constant temperature method proposed by Woodcock [15] and somewhat modified by us [16]; that is, a common factor instead of individual factors is applied to the different species at each step. In a few runs, a constant energy procedure was also performed in order to check that the constant temperature procedure yields reasonable dynamical properties.

The masses of the ions were drastically changed, as has often been done in this kind of MD [17–19]. The Ewald method [20] was used for the calculation of the coulombic forces; the cut distance in real space was  $L/2$ , and the reciprocal lattice vectors  $|\mathbf{n}|^2$  were counted up to 27. The runs are numbered as in Table 1, where the pressure obtained from the

Reprint requests to Dr. Isao Okada, Department of Electronic Chemistry, Tokyo Institute of Technology, Nagatsuta 4259, Midori-ku, Yokohama 227, Japan.

0340-4811 / 84 / 0900-0880 \$ 01.30/0. – Please order a reprint rather than making your own copy.



Dieses Werk wurde im Jahr 2013 vom Verlag Zeitschrift für Naturforschung in Zusammenarbeit mit der Max-Planck-Gesellschaft zur Förderung der Wissenschaften e.V. digitalisiert und unter folgender Lizenz veröffentlicht: Creative Commons Namensnennung-Keine Bearbeitung 3.0 Deutschland Lizenz.

Zum 01.01.2015 ist eine Anpassung der Lizenzbedingungen (Entfall der Creative Commons Lizenzbedingung „Keine Bearbeitung“) beabsichtigt, um eine Nachnutzung auch im Rahmen zukünftiger wissenschaftlicher Nutzungsformen zu ermöglichen.

This work has been digitalized and published in 2013 by Verlag Zeitschrift für Naturforschung in cooperation with the Max Planck Society for the Advancement of Science under a Creative Commons Attribution-NoDerivs 3.0 Germany License.

On 01.01.2015 it is planned to change the License Conditions (the removal of the Creative Commons License condition “no derivative works”). This is to allow reuse in the area of future scientific usage.

Table 1. Run number of MD and the calculated pressures.

	Mass		950 K		1100 K		1250 K	
	Li	Cl	No.	<i>P</i> /GPa	No.	<i>P</i> /GPa	No.	<i>P</i> /GPa
Isotopically pure salt	6.941	35.453	PA1	0.14	PA2	0.21	PA3	0.17
							EPA3	0.17
							(1245 K)	
	22.98977	35.453	PB1	0.24	PB2	0.11	PB3	0.17
	14.965	35.453			PC2	0.14		
Isotopic mixture	6.941	126.9045	PD1	0.11	PD2	0.17		
	{ 6.941 {54} 22.98977 {54} }	35.453	MA1	0.17	MA2	0.18	MA3	0.18
					EMA2	0.21		
					(1178 K)			
	{ 6.941 {8} 22.98977 {100} }	35.453			MB2	0.22		
	{ 6.941 {54} 22.98977 {54} }	126.9045			MC2	0.22		

EPA3 and EMA2 are constant-energy runs, whose densities are fixed at the temperatures specified at the top of column; the obtained average temperature is given in parentheses. The numbers in braces represent the numbers of ions in the basic cell.

Table 2. Position of some characteristic points of the pair correlation functions of molten LiCl.

		950 K	1100 K	1250 K
$g_{\text{Li-Cl}}$	$R_0$	170	164	164
	$R_M$	221 (0.92)	221 (0.93)	221 (0.94)
	$R_i$	244 (2.01)	244 (1.95)	244 (1.87)
	$R_2$	282 (3.15)	282 (3.02)	282 (2.90)
	$R_m$	350 (4.20)	350 (4.08)	350 (3.97)
$g_{\text{Li-Li}}$	$R_0$	244	240	238
	$R_M$	373	375	375
	$R_m$	520	530	530
$g_{\text{Cl-Cl}}$	$R_0$	278	272	270
	$R_M$	371	368	375
	$R_m$	530	530	520

The distances are given in pm. The numbers in parentheses indicate the coordination number for the distance given just before it.

virial [21] is also given. Most of the runs comprised about 3000 time steps after attainment of equilibrium. At the same temperature and density the pressure must be the same, independent of the masses of the constituent ions; the fact that this does

not necessarily hold suggests that the number of time-steps was not sufficient for the calculation of the pressure.

### III. Results and Discussion

#### A) Structure

The pair correlation functions at 1100 K are shown in Fig. 1; they are identical within statistical uncertainties for the runs PA2, PB2, PC2 and PD2. Also at other temperatures, the pair correlation functions are independent of the ionic masses as is to be expected, since in classical mechanics the equilibrium state is independent of the masses.

In LiCl, the pair correlation functions  $g_{++}$  and  $g_{--}$  are distinctly different at short distances, as already pointed out by a Monte Carlo simulation [11].  $g_{++}$  starts to rise at a shorter distance than does  $g_{--}$  because  $\sigma_{\text{Li}}^0$  is much smaller than  $\sigma_{\text{Cl}}^0$ , and the first peak is lower for  $g_{++}$  than for  $g_{--}$ . This is in contrast to other salts such as NaCl [22] and KCl

[23] where  $g_{++}$  and  $g_{--}$  are almost equal.  $R_i$  is the position of the inflection point after the first peak.  $R_2$  may be regarded as the end of the nearest neighbour interaction [24]. Table 2 gives the position of the characteristic points (cf. Fig. 1) of the pair correlation functions. The positions of  $R_M$ ,  $R_i$  and  $R_2$  are practically independent of temperature in the investigated temperature range (950 K–1250 K). This insensitivity to temperature can also be seen from the angular correlation as stated in the following.

For more insight into the short-range structure, the triplet distribution function [25]

$$h_{+-+}(<R_2, <R_2, \cos \theta) = \frac{dn}{N \sin \theta d\theta} \quad (2)$$

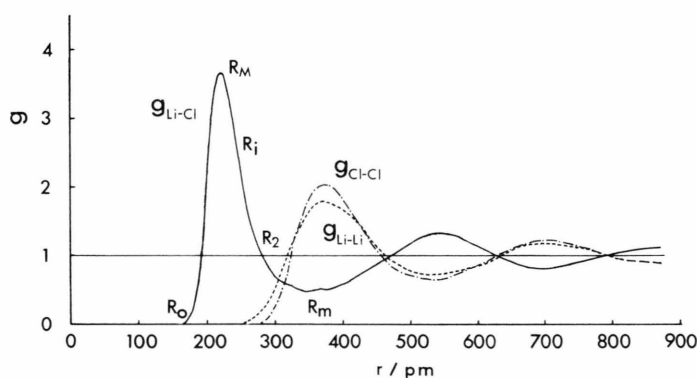


Fig. 1. Pair correlation functions at 1100 K.

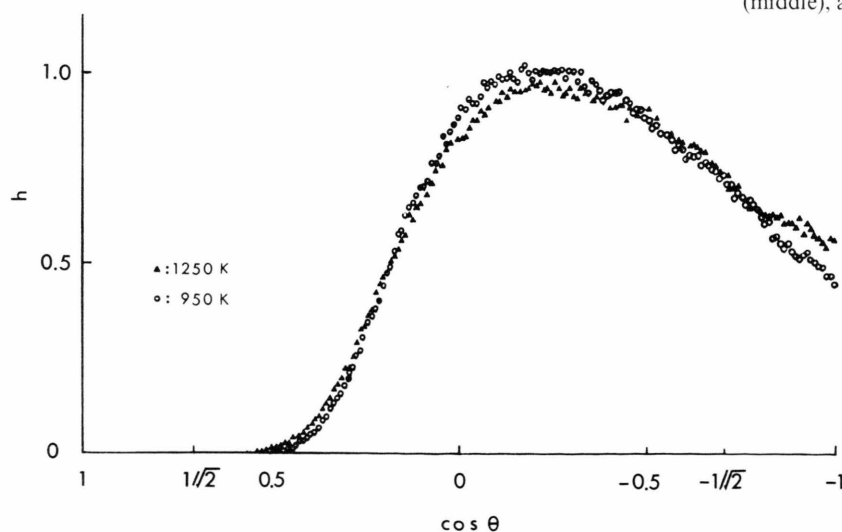


Fig. 2. Angular distribution functions,  $h_{+-+}$ , for  $\text{Li}^+$  ions centred on a  $\text{Cl}^-$  ion with  $R_2$ .

of two  $\text{Li}^+$  ions coordinated to a  $\text{Cl}^-$  ion within  $R_2$  has been evaluated, where  $n/N$  is the running relative frequency and  $\int_{-1}^1 h d \cos \theta = 1$ . The results for 950 K and 1250 K are shown in Fig. 2. The curve is only slightly sharper for 950 K than for the 1250 K. The peak is located at  $\cos \theta = -0.25$ , which corresponds to  $\theta = 105^\circ$ . This indicates that most of the  $\text{Li}^+$  ions coordinate nearly tetrahedrally to a  $\text{Cl}^-$  ion.

The distribution of the numbers of  $\text{Li}^+$  ions coordinating to a  $\text{Cl}^-$  ion within  $R_2 = 282$  pm is depicted in Fig. 3; the coordination number thus defined is peaked at 3 with a probability of about 0.55 almost independent of temperature. The second probable coordination number depends on temperature, i.e. 4 at 950 K and 2 at 1250 K. As temperature increases,

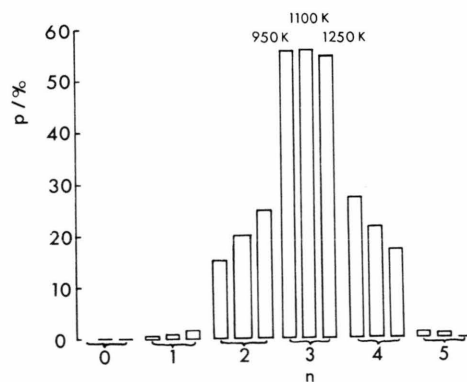


Fig. 3. Distribution of coordination numbers of unlike ions within  $R_2$  at 950 K (left), 1100 K (middle), and 1250 K (right).

Table 3. Self-exchange velocities ( $\text{m s}^{-1}$ ).

	Mass		950 K	1100 K	1250 K
	Li	Cl			
Isotopically pure salt	6.941	35.453	134.7 (PA1)	171.1 <sup>a</sup> (PA2)	207.6 (PA3)
	22.98977	35.453	98.9 (PB1)	124.0 (PB2)	206.8 (EPA3)
	14.965	35.453		143.9 (PC2)	150.5 (PB3)
	6.941	126.9045	93.0 (PD1)	117.1 (PD2)	
Isotopic mixture	{ 6.941 {54}	35.453	118.4	153.0	195.9
			103.6 (MA1)	131.6 (MA2)	163.7 (MA3)
	{ 22.98977 {54}	35.453		171.6 (EMA2)	
				149.1	
	{ 6.941 {8}	35.453		158.5	
				127.5 (MB2)	
	{ 22.98977 {100}	35.453			
	{ 6.941 {54}	126.9045		113.5	
				90.7 (MC2)	
	{ 22.98977 {54}	126.9045			

<sup>a</sup> In a previous study [5], this was evaluated to be  $165 \text{ m s}^{-1}$ ; however, the present value should be more accurate owing to better statistics. See also the footnote to Table 1. The numbers in braces represent the numbers of ions in the periodic cube.

the volume of free space increases, which will make the average coordination number lower; the average coordination numbers are 3.15, 3.02 and 2.90 at 950 K, 1100 K and 1250 K, respectively.

### B) Self-exchange velocity

#### B-1) Relation between SEV and internal mobility

The separating motion of unlike ion pairs can be expressed in terms of the self-exchange velocity (SEV) which is defined as [5]

$$v(d_1, d_2) = \frac{(d_2 - d_1)}{\tau}, \quad (3)$$

where  $d_1 = \bar{R}_2$  is the average of the distances  $< R_2$  of the unlike particles at zero time and  $d_2 = R_2$  is the average distance of the same individual particles at the time  $\tau$ .

The values of  $v$  are calculated for  $\text{Li}^+$  ions surrounding totally 6480  $\text{Cl}^-$  ions and 12960  $\text{Cl}^-$  ions in the isotopically pure and mixed LiCl, respectively.

The calculated values of  $v(\bar{R}_2, R_2)$  are tabulated in Table 3. The values obtained with the usual con-

stant energy procedure agree with those derived with our constant temperature procedure in case of EPA3, and the former are compatible with the latter also in case of EMA2, if the actual temperature of this constant energy run is taken into account.

In order to check for the correlation between the mobility and the SEV, the experimental molar conductivity  $\Lambda$  of LiCl melt as recommended in [14], which reaches from 910 K up to 1050 K, has to be extrapolated. One obtains with sufficient accuracy  $203 \pm 2 \text{ S cm}^2 \text{ mol}^{-1}$  and  $229 \pm 2 \text{ S cm}^2 \text{ mol}^{-1}$  for 1100 K and 1250 K, respectively.

In Fig. 4, some SEV's obtained with the 'natural masses' of the  $\text{Li}^+$  and  $\text{Cl}^-$  ions (PA1, PA2 and PA3), are plotted against the internal mobilities  $b = \Lambda/F$  for three temperatures. It is seen that they are all correlated with  $b$ . The straight line of  $v(\bar{R}_2, R_2)$  vs.  $b$ , however, does not pass through the origin, as opposed to our previous expectation [5, 6]. This straight line is calculated to be

$$v(\bar{R}_2, R_2) = (1.29 \pm 0.03) \times 10^9 b - (100.0 \pm 5.5), \quad (b \text{ in } \text{m}^2 \text{ s}^{-1} \text{ V}^{-1}; v \text{ in } \text{m s}^{-1}). \quad (6)$$

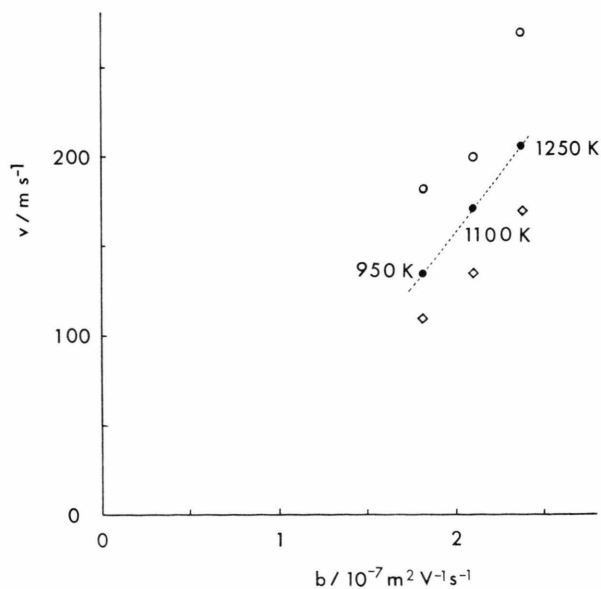


Fig. 4. Relation between  $v$  and  $b$ . ○:  $v(\bar{R}_1, R_2)$ , ●:  $v(\bar{R}_2, R_2)$ , ◇:  $v(\bar{R}_m, R_m)$ .

For  $v(\bar{R}_1, R_2)$  the statistics is worse than for  $v(\bar{R}_2, R_2)$  because of the small coordination number within  $R_1$ , and in case of  $v(\bar{R}_m, R_m)$  it is generally hard to define the position of  $R_m$  since the minimum is flat. Therefore  $v(\bar{R}_2, R_2)$  is taken as the SEV to be discussed.

## B-2) The motion of a cation around an anion

In Fig. 5, the time evolution in a 1:1 mixture at 950 K (MA1) of the distances of four individual  $\text{Li}^+$  ions located within  $R_2$  at  $t=0$  from an arbitrarily chosen  $\text{Cl}^-$  ion is shown. As seen from Fig. 5, the motion of the  $\text{Li}^+$  ions with reference to the adjacent  $\text{Cl}^-$  ions can be classified into 3 modes: (1) an oscillating motion (O-process), (2) a leaving motion (L-process) and (3) a coming-back motion which sometimes occurs following soon after the leaving motion (C-process).

The average duration of the O-process is evaluated here in terms of the time  $\tau_H$  in which the number

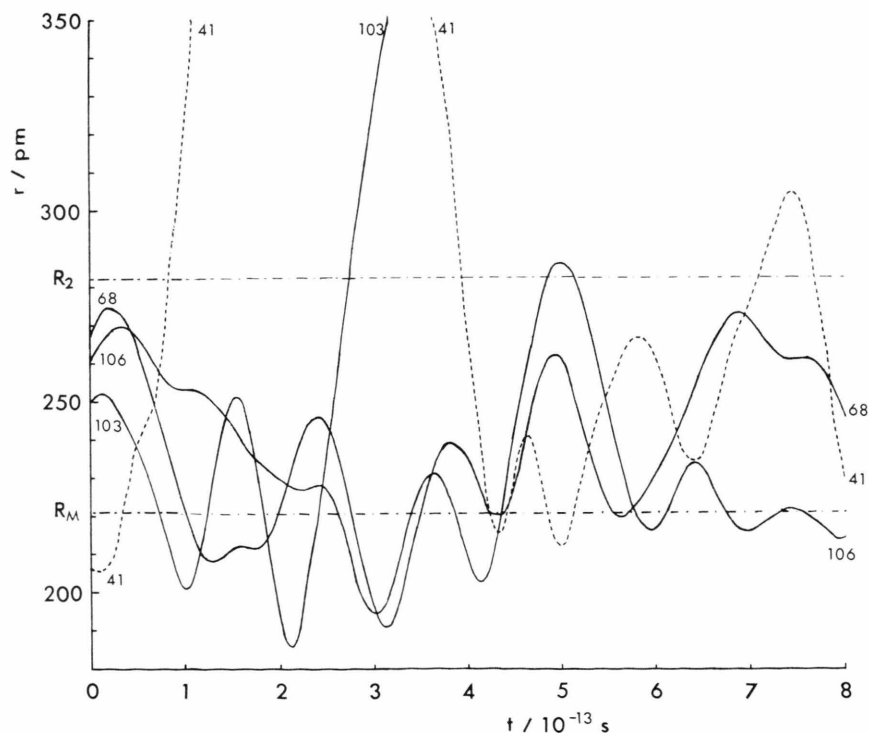


Fig. 5. Time evolution of distances of  $\text{Li}^+$  ions from an arbitrarily chosen  $\text{Cl}^-$  ion (MA1). Numbers refer to the number of the  $\text{Li}^+$  ion (No. 41:  $M_{\text{Li}} = 6.941$ , Nos. 68, 103 and 106:  $M_{\text{Li}} = 22.98977$ ).

Table 4. Average durations,  $\tau_H$ , for half of the marked neighbouring  $\text{Li}^+$  ions to leave the coordination sphere ( $R_2$ ) around a  $\text{Cl}^-$  ion (in ps), and  $\tau_H$  ratios.

	Mass <sup>a</sup>		950 K	1100 K	1250 K
	Li	Cl			
Isotopically pure salts	7	35.5	0.931 (PA1)	0.752 (PA2)	0.600 (PA3)
	23	35.5	1.30 (PB1)	1.04 (PB2)	0.819 (PB3)
	7	127	1.5 <sup>b</sup> (PD1)	1.05 (PD2)	
Isotopic 1:1 mixtures	7	35.5	1.13 (MA1)	0.869 (MA2)	0.633 (MA3)
	23	35.5	1.22 (MA1)	0.901 (MA2)	0.714 (MA3)
	7	127		1.13 (MC2)	
$\tau_H(23, 35.5)/\tau_H(7, 35.5)$			1.40 (PA1–PB1)	1.38 (PA2–PB2)	1.37 (PA3–PB3)
$\tau_H(23, 35.5)/\tau_H(7, 35.5)$			1.08 (MA1)	1.04 (MA2)	1.13 (MA3)
$\tau_H(23, 127)/\tau_H(7, 127)$				1.09 (MC2)	

<sup>a</sup> Approximate masses.  
<sup>b</sup> Extrapolated value from  $t \leq 1.2$  ps.

Table 5. Separating speeds,  $v_L$ , of unlike ion pairs in the L-process (in  $\text{m s}^{-1}$ ), and  $v_L$  ratios.

	Mass		950 K	1100 K	1250 K
	Li	Cl			
Isotopically pure salts	7	35.5	$1462 \pm 50$ (PA1)	$1591 \pm 51$ (PA2)	$1673 \pm 51$ (PA3)
	23	35.5	$1061 \pm 41$ (PB1)	$1144 \pm 42$ (PB2)	$1190 \pm 41$ (PB3)
	7	127	$1252 \pm 25$ (PD1)	$1346 \pm 20$ (PD2)	
Isotopic 1:1 mixtures	7	35.5	$1443 \pm 69$ (MA1)	$1571 \pm 74$ (MA2)	$1629 \pm 70$ (MA3)
	23	35.5	$1099 \pm 58$ (MA1)	$1154 \pm 58$ (MA2)	$1226 \pm 57$ (MA3)
	7	127		$1352 \pm 29$ (MC2)	
$v_L(7, 35.5)/v_L(23, 35.5)$			$1.379 \pm 0.071$ (PA1–PB1)	$1.391 \pm 0.068$ (PA2–PB2)	$1.406 \pm 0.065$ (PA3–PB3)
$v_L(7, 35.5)/v_L(23, 35.5)$			$1.313 \pm 0.094$ (MA1)	$1.361 \pm 0.094$ (MA2)	$1.329 \pm 0.084$ (MA3)
$v_L(7, 127)/v_L(23, 127)$				$1.528 \pm 0.049$ (MC2)	

of the marked cations within  $R_2$  becomes half the initial one. The values of  $\tau_H$  and the ratios of two isotopes in some runs are given in Table 4.

The average speed in the L-process is calculated over the distance between 282 pm and 350 pm for about 4000 unlike ion pairs. The average speeds are given in Table 5 together with the standard deviations.

The fact that the isotope effect for the duration of the O-process in the mixture is small indicates that the initiation of the L-process is more strongly affected by the surrounding ions than by the own motion of an unlike ion pair of interest.

B-3) The mass dependence of SEV's and experimental internal mobilities

The ratio of the mobilities of two isotopes in a gaseous, completely dissociated salt is given by the inverse ratio of the respective reduced masses of the cation-anion pairs. If the reduced mass of  $^7\text{Li}$  and natural chlorine is chosen as reference, we are concerned with the ratios

$$\varphi = \sqrt{\frac{M_{\text{Li}} + M_{\text{Cl}}}{M_{\text{Li}} M_{\text{Cl}}}} / \sqrt{\frac{7 + 35.5}{7 \times 35.5}} \quad (5)$$

Table 6. Values of  $\beta$  and  $\psi$  defined in (6) and (7).

	950 K	1100 K	1250 K
$\beta$	1.0545	1.0578	1.0611
$\langle 0.925 \rangle \beta$	1.0198	1.0252	1.0320
$\psi (23, 35.5)$	0.734	0.725	0.725
$\psi (15, 35.5)$		0.841	
$\psi (7, 127)$	0.691	0.729	
$\langle 0.5 \rangle \psi$	0.875	0.860	0.836
$\langle 0.925 \rangle \psi$		0.804	

The numbers in angle brackets are the mole fractions of the heavier Li isotopes in the mixtures.  $\beta$  and  $\psi$  not specified by angle brackets correspond to isotopically pure salts.

The experimental mobility ratios

$$\beta = b(6, 35.5)/b(7, 35.5) \quad (6)$$

are closer to unity (no isotope effect) than  $\varphi$ , and the corresponding SEV ratios

$$\psi = v(M_{\text{Li}}, M_{\text{Cl}})/v(7, 35.5) \quad (7)$$

should also be closer to unity than  $\varphi$ . The available values of  $\beta$  (Ref. [4]) and  $\psi$  (as obtained from Table 3) are collected in Table 6 and presented graphically in Figure 6.

Most of the points are situated between the diagonal, which corresponds to an upper limit for the isotope effects, and the horizontal  $\beta = \psi = 1$ , which corresponds to zero isotope effect. The points belonging to  $\psi(7, 127)$  lie outside this range. This needs clarification. As far as the mass of the  $\text{Cl}^-$  ion is 35.5, a nice correlation between the  $\beta$ - and  $\psi$ -values is found.

#### B-4) The isotope effect of SEV's in pure and mixed melts

Figure 6 shows that, for the SEV's as well as the internal mobilities, the isotope effects between isotopically pure salts are larger than those within isotope mixtures.

In order to explain the behaviour of the mobilities in binary melts of chemically different cations with a common anion, we have assumed an agitation effect on the larger cations by the smaller and lighter spectator cations [26, 27]. This effect can be made clearer in the present study:

The fast (slow) motion of light (heavy) spectator  $\text{Li}^+$  ions, if present in the melt, shortens (lengthens) the duration of the O-process for the heavy (light)

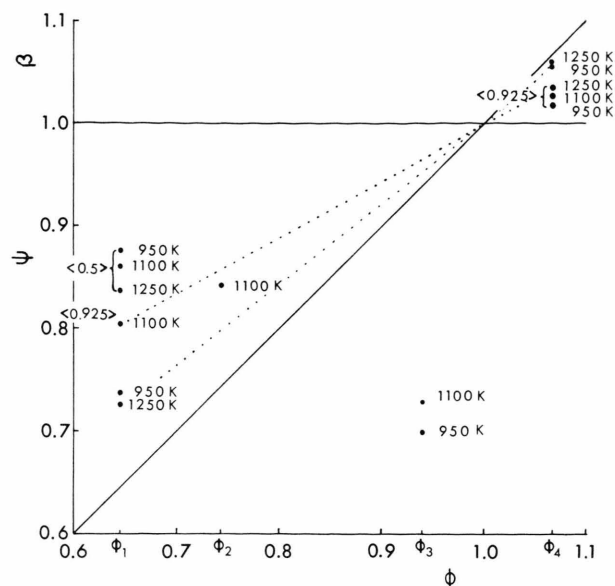


Fig. 6. Values of  $\beta$  and  $\psi$  vs.  $\varphi$ . The numbers in angle brackets are the mole fractions of the heavier Li isotope. Points not preceded by brackets correspond to isotopically pure salts.  $\varphi_1 = \varphi(23, 35.5) = 0.645$ ,  $\varphi_2 = \varphi(15, 35.5) = 0.743$ ,  $\varphi_3 = \varphi(7, 127) = 0.939$ ,  $\varphi_4 = \varphi(6, 35.5) = 1.067$ .

$\text{Li}^+$  ions, as can be seen in Table 4. These “agitation” and “tranquillisation” effects correspond to what has been called the “drag” effect by Klemm [28] and explain the large isotope effects between isotopically pure melts as compared to those within isotopic mixtures.

#### B-5) The temperature dependence of the isotope effect of SEV's

As is also seen from Fig. 6, the isotope effects of the  $\text{Li}^+$  ions increase with temperature. This is because with increasing temperature the O-process, in which the isotope effect is generally smaller than in the L-process (see Tables 4 and 5), becomes shorter.

The increase of the isotope effects with temperature is greater for the mixtures than for the isotopically pure salts. This corresponds to the fact that the O-process, in which the isotope effect is considerably smaller within the mixtures than between the isotopically pure salts, becomes shorter with temperature, as seen from Table 4.

As for the self-diffusion coefficients, the effect of the mass in molten LiBr has been elegantly interpreted with the perturbation theory by Lantelme et al. [29].



In conclusion, the following trends experimentally obtained for internal mobilities of molten LiCl [4] have been reflected by the SEV's:

- (1) The isotope effects between the isotopically pure salts are larger than between the isotopes within isotopic mixtures.
- (2) The isotope effects increase with temperature.
- (3) The increase with temperature is larger for the mixtures than for the isotopically pure salts.

The agitation and tranquillisation effects could be clearly recognized and correlated with the reduced isotope effects of the SEV's within isotopic mixtures.

The author is much indebted to Professor A. Klemm for invaluable suggestions particularly in the section of the mass dependence.

The calculation was performed with a HITAC M-200 computer at the Computer Centre, Institute for Molecular Science. The computer time made available for this study is gratefully acknowledged.

- [1] A. Klemm, H. Hintenberger, and P. Hoernes, *Z. Naturforsch.* **2a**, 245 (1947).
- [2] A. Klemm and E. U. Monse, *Z. Naturforsch.* **12a**, 319 (1957).
- [3] R. Lenke and A. Klemm, *Z. Naturforsch.* **20a**, 1723 (1965).
- [4] S. Jordan, R. Lenke, and A. Klemm, *Z. Naturforsch.* **23a**, 1563 (1968).
- [5] I. Okada, R. Takagi, and K. Kawamura, *Z. Naturforsch.* **35a**, 493 (1980).
- [6] I. Okada and R. Takagi, *Z. Naturforsch.* **36a**, 378 (1981).
- [7] G. Ciccotti, G. Jacucci, and I. R. McDonald, *Phys. Rev.* **A13**, 426 (1976).
- [8] A. Klemm, *Z. Naturforsch.* **32a**, 927 (1977).
- [9] M. Harada, A. Yamanaka, M. Tanigaki, and Y. Tada, *J. Chem. Phys.* **76**, 1550 (1982).
- [10] M. P. Tosi and F. G. Fumi, *J. Phys. Chem. Solids* **25**, 45 (1964).
- [11] J. W. E. Lewis, K. Singer, and L. V. Woodcock, *J. Chem. Soc. Faraday Trans. II* **71**, 301 (1975).
- [12] H. Ohno, M. Yoroki, K. Furukawa, Y. Takagi, and T. Nakamura, *J. Chem. Soc. Faraday Trans. I* **74**, 1861 (1978).
- [13] I. Okada, H. Okano, H. Ohtaki, and R. Takagi, *Chem. Phys. Lett.* **100**, 436 (1983).
- [14] G. J. Janz, F. W. Dampier, G. R. Lakshminarayanan, P. K. Lorenz, and R. P. T. Tomkins, *Molten Salts: Vol. 1, Electrical Conductance, Density, and Viscosity Data*, NSRDS-NBS 15, Nat. Bur. Stand. Washington 1968.
- [15] L. V. Woodcock, *Chem. Phys. Lett.* **10**, 257 (1971).
- [16] I. Okada, Y. Matsui, and K. Kawamura, *Nippon Kagaku Kaishi* **1982**, 910.
- [17] F. Lantelme, P. Turq, and P. Schofield, *J. Chem. Phys.* **67**, 3869 (1977).
- [18] F. Lantelme, P. Turq, and P. Schofield, *J. Chem. Phys.* **71**, 2507 (1979).
- [19] F. Lantelme, *Mol. Phys.* **47**, 1277 (1982).
- [20] P. P. Ewald, *Ann. Phys.* **64**, 253 (1921).
- [21] L. Schäfer and A. Klemm, *Z. Naturforsch.* **31a**, 1068 (1976).
- [22] F. Lantelme, P. Turq, B. Quentrec, and J. W. E. Lewis, *Mol. Phys.* **28**, 1537 (1974).
- [23] L. V. Woodcock and K. Singer, *Trans. Faraday Soc.* **67**, 12 (1971).
- [24] G. Pálkás, W. O. Riede, and K. Heinzinger, *Z. Naturforsch.* **32a**, 1137 (1977).
- [25] L. Schäfer and A. Klemm, *Z. Naturforsch.* **34a**, 993 (1979).
- [26] C. Yang, R. Takagi, and I. Okada, *Z. Naturforsch.* **35a**, 1186 (1980).
- [27] C. Yang, R. Takagi, and I. Okada, *Z. Naturforsch.* **38a**, 135 (1983).
- [28] A. Klemm, *Z. Naturforsch.* **39a**, 471 (1984).
- [29] F. Lantelme and P. Turq, *Mol. Phys.* **38**, 1003 (1979).